

An ancient F-type subdwarf from the halo crossing the Galactic plane[★]

R.-D. Scholz¹, U. Heber², C. Heuser², E. Ziegerer², S. Geier³, and F. Niederhofer³

¹ Leibniz Institute for Astrophysics Potsdam (AIP), An der Sternwarte 16, 14482 Potsdam, Germany e-mail: rdscholz@aip.de

² Dr. Remeis Observatory & ECAP, Astronomical Institute, Friedrich-Alexander University Erlangen-Nürnberg, Sternwartstr. 7, 96049 Bamberg, Germany

³ European Southern Observatory, Karl-Schwarzschild-Str. 2, 85748 Garching, Germany

Received 5 December 2014; accepted 19 December 2014

ABSTRACT

Aims. We selected the bluest object, WISE J0725–2351, from Luhman’s new high proper motion (HPM) survey based on observations with the Wide-field Infrared Survey Explorer (WISE) for spectroscopic follow-up observations. Our aim was to unravel the nature of this relatively bright ($V \sim 12$, $J \sim 11$) HPM star ($\mu = 267$ mas/yr).

Methods. We obtained low- and medium-resolution spectra with the European Southern Observatory (ESO) New Technology Telescope (NTT)/EFOSC2 and Very Large Telescope (VLT)/XSHOOTER instruments, investigated the radial velocity and performed a quantitative spectral analysis that allowed us to determine physical parameters. The fit of the spectral energy distribution based on the available photometry to low-metallicity model spectra and the similarity of our target to a metal-poor benchmark star (HD 84937) allowed us to estimate the distance and space velocity.

Results. As in the case of HD 84937, we classified WISE J0725–2351 as sdF5: or a metal-poor turnoff star with $[Fe/H] = -2.0 \pm 0.2$, $T_{eff} = 6250 \pm 100$ K, $\log g = 4.0 \pm 0.2$, and a possible age of about 12 Gyr. At an estimated distance of more than 400 pc, its proper motion translates to a tangential velocity of more than 500 km/s. Together with its constant (on timescales of hours, days, and months) and large radial velocity (about +240 km/s), the resulting Galactic restframe velocity is about 460 km/s, implying a bound retrograde orbit for this extreme halo object that currently crosses the Galactic plane at high speed.

Key words. Proper motions – Stars: distances – Stars: kinematics and dynamics – Stars: Population II – subdwarfs – white dwarfs

1. Introduction

Most of the roughly 50000 known high proper motion (HPM) stars (with $\mu \gtrsim 0.2$ arcsec/yr) were detected in optical surveys based on photographic Schmidt plates (e.g. by Luyten 1979a, 1979b, Scholz et al. 2000, Pokorny et al. 2004, Hambly et al. 2004, Lépine & Shara 2005, Lépine 2005, 2008). The majority of these HPM stars are not high velocity, but just nearby ($2 \lesssim d \lesssim 50$ pc) stars that belong to the thin disc and the same spiral arm as the sun. However, among the HPM stars there are also few thick disc and even fewer Galactic halo stars (subdwarfs) that are on average several times further away ($10 \lesssim d \lesssim 250$ pc), but cross the solar neighbourhood at high speeds (with tangential velocities of up to several 100 km/s). Therefore, the proper motion alone can only provide a crude distance estimate. Nevertheless, it is often used as a starting point in the search for unknown nearby stars.

The incompleteness of the census of nearby stars, dominated by M dwarfs, increases with distance, as demonstrated for the northern and southern hemispheres, respectively by Lépine & Gaidos (2013) and Winters et al. (2014). For the immediate solar neighbourhood, the Research Consortium on Nearby Stars (RECONS)¹ gives regular updates for a high-quality 10 pc sample. All systems in that sample have trigonometric parallaxes with

errors of less than 10 mas. From 2000 to 2012, the numbers of M dwarfs in this sample increased from 198 to 248 (by 25%), whereas the number of white dwarfs (WDs) rose from 18 to 20 (by about 10%). This progress was achieved thanks to RECONS and other parallax programmes that concentrated on previously detected new HPM objects. Adric Riedel and the RECONS team also provided the numbers of known systems and different types of objects in the 15.625 times larger volume of the 25 pc sample in a video of 12 June 2014. The numbers of M dwarfs (1093) and WDs (137) announced in this video are two-three times smaller than the expected numbers (~ 3900 and ~ 310 , respectively), if one assumes that the number densities do not change from 10 to 25 pc. This demonstrates the potential for the identification of hitherto unknown WD and M dwarf neighbours of the sun and the need for ongoing and new parallax programmes. Concerning nearby WDs, there is an interesting lack of moderately HPM objects: 100% of the known WDs within 10 pc have total proper motions > 500 mas/yr and 84% have > 1000 mas/yr, whereas for other stars these fractions are only 81% and 49%, respectively (data from SIMBAD). We suspect that some nearby WDs with relatively small proper motions have not yet been identified.

We note that only four subdwarfs (LHS 29, LHS 189, LHS 272, and LHS 406) are included in the above-mentioned video on the 25 pc sample, and all these are M-type subdwarfs. The late-M subdwarf SSSPM J1444–2019 (Scholz et al. 2004) with a parallax of 61.67 ± 2.12 mas (Schilbach et al. 2009) should be added here. Jao et al. (2008) reported in their Table 2 on some additional subdwarfs possibly falling in the 25 pc sam-

[★] Based on observations at the La Silla-Paranal Observatory of the European Southern Observatory for programmes 092.D-0040(A) and 093.D-0127(A).

¹ <http://www.chara.gsu.edu/RECONS/>

ple (with $K_s - M_{K_s} \lesssim 2$; see also Table 4 of Winters et al. 2014). They also mentioned (in their Sect. 7.2.2) the nearest subdwarf binary μ Cas AB (listed in SIMBAD with a spectral type of "K1V_Fe-2") with an accurate parallax of 132.38 ± 0.82 mas (van Leeuwen 2007). Another K-type subdwarf binary possibly within 25 pc is LHS 72/73 (Reyl   et al. 2006, Jao et al. 2008, Rajpurohit et al. 2014). As in the case of main-sequence dwarfs, K- and especially M-type subdwarfs are much more frequent in the solar neighbourhood than earlier-type subdwarfs. The nearest known F- and G-type subdwarfs with trigonometric parallaxes lie according to SIMBAD slightly beyond 50 pc. Concerning A-type subdwarfs, there is no clear evidence for their existence. Besides some historical papers on this topic (Chamberlain & Aller 1951, Greenstein 1954), we found only two A-type subdwarfs with trigonometric parallaxes in SIMBAD (corresponding to distances >180 pc). One of those (HD 224927) is a close binary with an A-type primary, whereas the other (HD 161817) is classified as a horizontal branch star. Their sdA8 and sdA2 types, respectively listed in SIMBAD, are both outdated as can be seen in the General Catalogue of Stellar Spectral Classifications (Skiff 2014).

The cool subdwarf sequence currently reaches from moderately cool F- to ultracool late-M-, L- and T-types and represents a completely different class of objects than hot O- and B-type subdwarfs. Their domains in a Hertzsprung–Russell diagram are clearly separated, as e.g. shown by Gontcharov et al. (2011), who called them unevolved and evolved subdwarfs, respectively. Jao et al. (2008) suggested using the "sd" prefix only for the hot evolved subdwarfs (sdO, sdB) and identifying all the cool unevolved subdwarfs by their luminosity class "VT". Drilling et al. (2013) presented a three-dimensional spectral classification (spectral, luminosity, and helium class) for the hot sdO and sdB subdwarfs. Over the last few decades, new classification systems were developed and refined for K- and M-type subdwarfs, with decreasing metallicity from normal subdwarfs (sd), to extreme (esd), and ultra (usd) subdwarfs (Gizis 1997, L  pine, Rich & Shara 2007). Many new ultracool subdwarfs have been discovered in recent years (see e.g. review by Burgasser et al. 2009, Cushing et al. 2009, Lodieu et al. 2012, Zhang et al. 2013, Wright et al. 2014, Kirkpatrick et al. 2014, Luhman & Sheppard 2014), whereas the warm end of the cool subdwarf sequence was not in the main focus of research (in terms of new discoveries and spectroscopic classification schemes).

Here, we report the identification and classification of a new F-type subdwarf crossing the Galactic plane at high speed. We selected this target as a rather blue and bright object in a new HPM survey and first suspected it to be a very nearby WD. (Sect. 2). In Sect. 3 and 4 we present our improved proper motion solution and the collected photometric data, respectively. Follow-up spectroscopic observations and radial velocity measurements are described in Sect. 5, whereas Sect. 6 deals with the spectral analysis. The distance and kinematics of the new halo object are estimated in Sect. 7. In Sect. 8 we give our conclusions and a brief discussion of our results.

2. Target selection

Multiple epochs from the Wide-field Infrared Survey Explorer (WISE; Wright et al. 2010), supplemented by about ten years older data from the Two Micron All Sky Survey (2MASS; Skrutskie et al. 2006), served as the basis for two new infrared HPM surveys (Luhman 2014a; Kirkpatrick et al. 2014) independent of photographic Schmidt plates. Both surveys aimed at the discovery of very nearby cool brown dwarfs (Luhman 2013, 2014a,

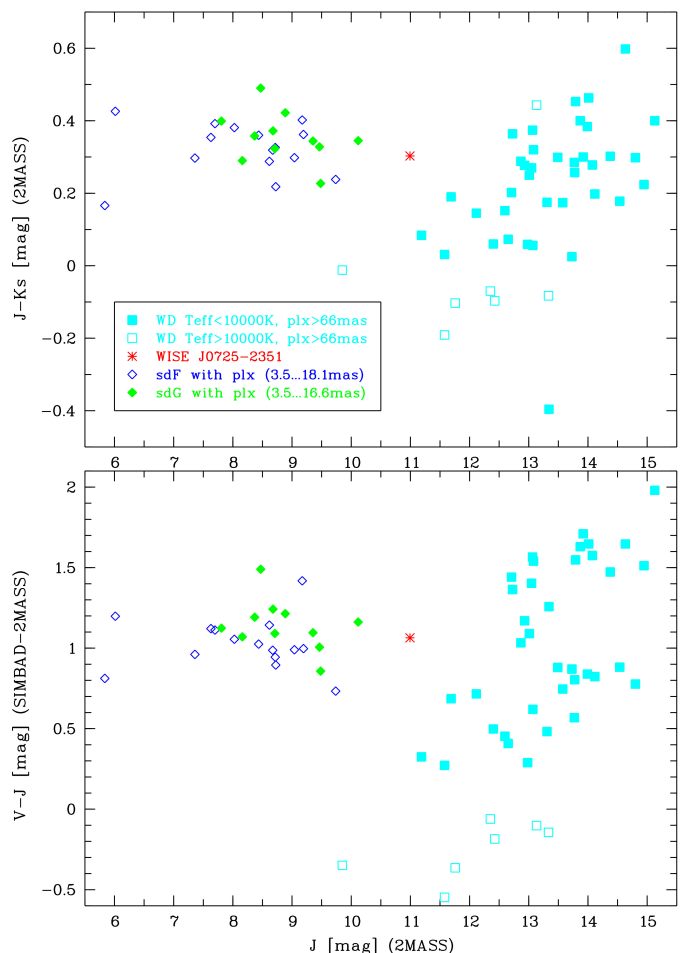


Fig. 1. Top: Near-infrared colour-magnitude diagram showing WISE J0725–2351 in comparison to nearby WDs and sdF/sdG subdwarfs with trigonometric parallaxes and available 2MASS photometry (close binaries excluded). **Bottom:** Optical-to-near-infrared colour-magnitude diagram showing the same objects.

2014b) and new L-type subdwarfs (Wright et al. 2014, Kirkpatrick et al. 2014, Luhman & Sheppard 2014). Among the new HPM objects of the Luhman (2014a) sample, there are also some blue objects, obviously overlooked in previous HPM surveys based on Schmidt plates. Among these sources, we selected the object with the AllWISE (Kirkpatrick et al. 2014) designation WISE J072543.88–235119.7 (hereafter WISE J0725–2351), also known as 2MASS J07254392–2351168, which had the smallest colour indices $J - w_2 = 0.35$ and $J - K_s = 0.30$, according to the 2MASS and WISE all-sky catalogue.

With these available colours and the bright magnitude ($J \sim 11.0$) we considered WISE J0725–2351 as a very nearby WD candidate and initiated spectroscopic follow-up observations (Sect. 5). However, we also mentioned that sdF and sdG subdwarfs have similar colours. In Fig. 1 (top) we compare the $J - K_s$ colour and J magnitude of our target with those of the known WDs within 15 pc (close binaries were excluded) and of all known sdF and sdG subdwarfs with available parallaxes as provided by SIMBAD. We are aware that these subdwarf samples may be not complete and may be contaminated with stars of different spectral and luminosity classes because of ambiguous classification or missing updates in SIMBAD. However, for both sdF and sdG in SIMBAD, their parallaxes range between about 3.5 mas and 19 mas, corresponding to distances between about 50 pc and 300 pc, where the relative errors of the smaller

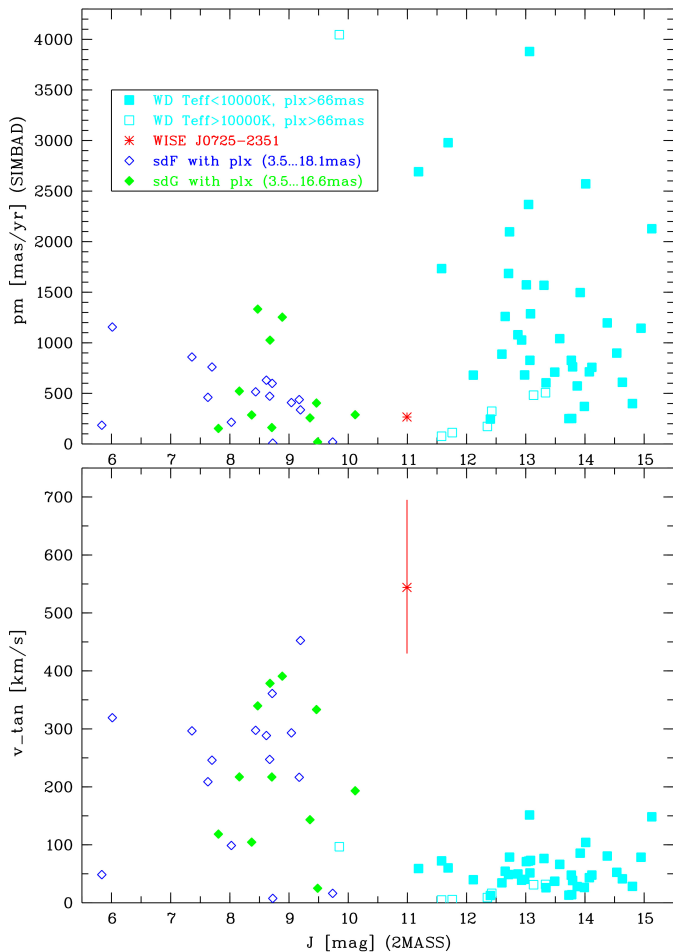


Fig. 2. Top: Proper motion as a function of J magnitude for WISE J0725–2351, nearby WDs, and sdF/sdG subdwarfs. **Bottom:** Tangential velocities based on the photometric distance estimate for WISE J0725–2351 (Sect. 7) and the trigonometric parallaxes of all other objects (same objects and symbols as in Fig. 1). For clarity, the error bars are shown for WISE J0725–2351 only. The error bars of sdF/sdG subdwarfs may be even larger in cases of uncertain parallaxes, whereas for WDs they are typically comparable to the symbol size.

parallaxes are very large. All but one of the WDs are fainter than WISE J0725–2351, whereas all the sdF and sdG with measured parallaxes are brighter. The $J-K_s$ colour of our target is consistent with that of the sdF, sdG, and the cool WDs. As we later found additional photometry for WISE J0725–2351 (Sect. 4), we include a $V-J, J$ diagram at the bottom of Fig. 1, where our target is again located between the regions occupied by sdF/sdG and cool WDs.

3. Improved proper motion

The relatively bright star WISE J0725–2351 was listed as a new HPM object in Luhman (2014a). It was not detected in any previous HPM survey. However, the PPM-Extended (PPMX; Röser et al. 2008) catalogue included this object with a somewhat different proper motion (Table 1), the United States Naval Observatory (USNO) B1.0 (Monet et al. 2003) associates a zero proper motion to this object, the Southern Proper Motion (SPM4; Girard et al. 2011) catalogue does not include this object, whereas the Fourth US Naval Observatory CCD Astrograph Catalog (UCAC4; Zacharias et al. 2013) gives only an accurate position but no proper motion. The reason for these discrepancies

Table 1. Proper motion of WISE J0725–2351

Source	$\mu_\alpha \cos \delta$ [mas/yr]	μ_δ [mas/yr]
Luhman (2014a)	-50 ± 10	-260 ± 10
AllWISE	-14 ± 36	-276 ± 36
USNO B1.0	0	0
PPMX	-74.1 ± 3.1	-265.3 ± 2.4
UCAC4	-	-
this work	-51.2 ± 1.7	-261.8 ± 0.8

is probably source confusion with a similarly bright blue background star (hereafter object B), with which our HPM star (object A) was almost overlapping at earlier epochs (see Fig. 3). Whereas both stars were resolved in the Tycho input catalogue (Egret et al. 1992), only the background object B entered the Tycho (ESA 1997) and Tycho-2 (Høg et al. 2000) catalogues (as TYC1 TYC2 TYC3 = 6538 2171 1, with non-significant proper motion components in Tycho-2 of less than 5 mas/yr). Both stars were included as a visual double star in the Washington double stars catalogue (Mason et al. 2001) with different separations (from 3.7 to 4.1 arcsec) and position angles (from 256° to 247°) measured between 1910 and 1922. This apparent double star was also catalogued as CD –23 5447 in the Cordoba Durchmusterung (Thome 1892)². Note that SIMBAD provides only one entry, CD –23 5447, within a few arcmin of the Tycho-2 star, but places it, probably because of the uncertain old input coordinates in the Cordoba Durchmusterung, at 07 25 44 –23 51.3 (ICRS coord), very close (within a few arcsec) to the current position of our HPM star.

For our improved proper motion solution (Table 1), we combined 14 available multi-epoch positions: the two mean WISE positions from 2010 (from AllWISE) and the 2MASS position from 1999 used by Luhman (2014a), the position from 1916 given in the Astrographic Catalogue (AC2000; Urban et al. 1998), our own visual measurement of the Digitized Sky Survey red plate from 1953 and the blue plate from 1980, five positions measured in the SuperCOSMOS Sky Survey (SSS; Hambly et al. 2001a, 2001c) and the SuperCOSMOS H_α survey (Parker et al. 2005) with epochs from 1980 to 2002, the 1999 position from UCAC4, the 2006 position from the last issue of the Carlsberg Meridian Catalogue (CMC15; Muñoz & Evans 2014), and the 2012 position measured by the Galaxy Evolution Explorer (GALEX³; Morrissey et al. 2007). The resulting proper motion of $(\mu_\alpha \cos \delta, \mu_\delta) = (-51.2 \pm 1.7, -261.8 \pm 0.8)$ is about two times more precise than the typical Tycho-2 proper motions of similarly bright stars in the field around WISE J0725–2351.

As seen in Fig. 2 (top), this proper motion represents a relatively small value for a nearby WD. If our target would have turned out to be a WD, it would have been a cool WD (see Fig. 1) within a few parsecs from the sun (according to its relatively bright magnitude). Its proper motion would translate to a very small tangential velocity (few km/s). Though this would be consistent with the majority of nearby WDs having tangential velocities between 0 and 100 km/s (Fig. 2, bottom). However, the opposite classification of WISE J0725–2351 as an F-type subdwarf (see Sect. 6) and its relatively faint magnitude with respect to the known objects of this class leads to a large distance (Sect. 7) and a very high tangential velocity (Fig. 2, bottom).

² <http://cdsarc.u-strasbg.fr/viz-bin/Cat?I/114>

³ <http://galex.stsci.edu/GR6/?page=mastform>

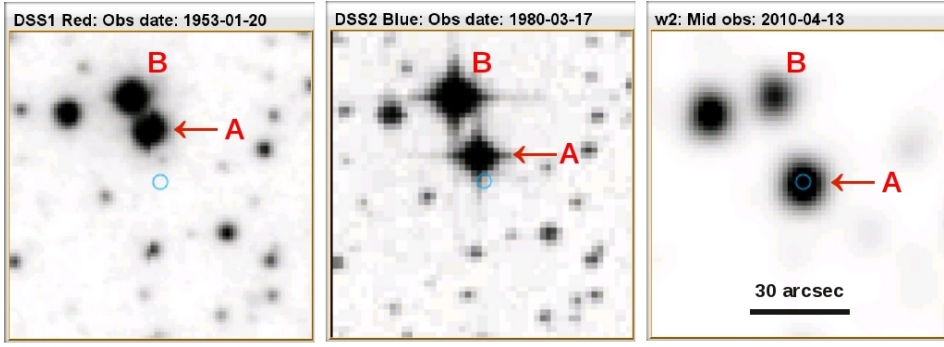


Fig. 3. Finder charts of 90×90 arcmin² (north is up, east to the left) from red and blue (first and second epoch, respectively) plates of the Digitized Sky Surveys (DSS) and from the WISE *w2*-band centred on the position of our HPM star WISE J0725–2351 (marked as object A) in the WISE all-sky catalogue (blue circle). At earlier epochs, our target moved very close to a blue background star (object B; see text).

Table 2. Photometry of WISE J0725–2351 and background object B

Source/ band	WISE J0725–2351 [mag]	object B [mag]
GALEX <i>NUV</i>	15.05 ± 0.01	13.81 ± 0.01
APASS <i>B</i>	12.482 ± 0.035	11.521 ± 0.035
Tycho <i>BT</i>	not available	11.239 ± 0.088
APASS <i>g'</i>	12.240 ± 0.029	11.436 ± 0.018
APASS <i>V</i>	12.057 ± 0.024	11.469 ± 0.023
Tycho <i>VT</i>	not available	11.193 ± 0.136
UCAC4 <i>f.mag</i>	11.984	11.545
APASS <i>r'</i>	11.960 ± 0.033	11.592 ± 0.024
CMC15 <i>r'</i>	11.919	11.549
APASS <i>i'</i>	11.819 ± 0.018	11.716 ± 0.005
2MASS <i>J</i>	10.993 ± 0.024	11.251 ± 0.026
2MASS <i>H</i>	10.720 ± 0.022	11.228 ± 0.022
2MASS <i>K_s</i>	10.690 ± 0.021	11.235 ± 0.023
AllWISE <i>w1</i>	10.616 ± 0.023	11.184 ± 0.024
AllWISE <i>w2</i>	10.644 ± 0.020	11.225 ± 0.020
AllWISE <i>w3</i>	10.612 ± 0.081	11.262 ± 0.148

4. Photometry

We collected the photometric data for WISE J0725–2351 and of the blue background star (object B in Fig. 3) from VizieR⁴ at the Centre de Données astronomiques de Strasbourg (CDS), the American Association of Variable Star Observers (AAVSO) Photometric all-sky survey (APASS)⁵ Data Release 7, and GALEX, as presented in Table 2. Note that the *r'* magnitudes from APASS and CMC15 (and the *f.mag* from UCAC4) are in very good agreement, respectively for both objects. We have not included the photographic SSS photometry (Hambly et al. 2001a, 2001b) in Table 2, as these relatively bright stars are affected by saturation and image crowding on the Schmidt plates.

With respect to our target WISE J0725–2351, the background object B appears blue, with all magnitudes from APASS *B* to AllWISE *w3* being in the range of about 11.2 to 11.7, whereas WISE J0725–2351 is nearly two magnitudes brighter in the mid-infrared WISE bands compared to the APASS *B*-band. According to its colour and small proper motion (Sect.3), object B could be an A star at a distance of ~ 700 –1600 pc (as derived from the comparison with the A7V star Altair and the A0V star Vega) with a tangential velocity of less than 16–38 km/s, which is typical of a thin disc star. Alternatively, object B could also be a B star (e.g. like the B7V star Regulus) but slightly reddened

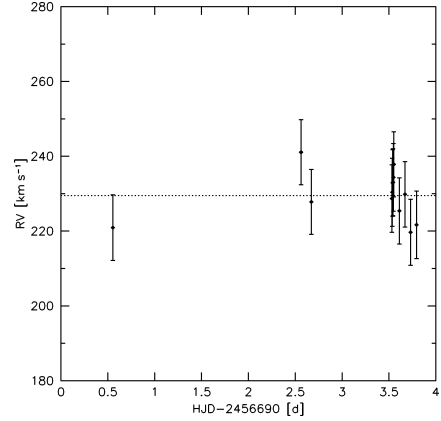


Fig. 4. Radial velocity measurements of WISE J0725–2351 from EFOSC2 spectra observed during three nights in February 2014. The dotted line shows the mean of these values.

($A_V \sim 0.2$). In that case it would lie at a distance of about 2500 pc with a tangential velocity of less than 60 km/s, which would still be realistic.

As shown in Fig. 1 for the *V*–*J* and *J*–*K_s* colours, WISE J0725–2351 appears similar to both sdF/sdG subdwarfs and cool WDs. Its $g' - r' = 0.28$ and $r' - i' = 0.14$ are consistent with the selection criteria for distant and much fainter ($r' > 15$) halo F-type stars used in Allende Prieto et al. (2014); and with $B - V = 0.43$, it is also similar to the nearby F5V star Procyon. However, with the absolute *V* magnitude of Procyon, WISE J0725–2351 would be about 780 pc away and consequently move at a tangential velocity of about 990 km/s, which is unlikely. An F-type subdwarf rather than a main-sequence star classification (Sect. 6) leads to a smaller distance and more realistic velocity (Sect. 7).

5. Spectroscopic observations, spectral classification, and radial velocity curve

To classify the star we obtained a low-resolution spectrum ($R \approx 700$, $\lambda = 3300$ –5200 Å) with the EFOSC2 spectrograph mounted at the European Southern Observatory (ESO) New Technology Telescope (NTT) in February 2014. Reduction was done with standard MIDAS procedures. The spectrum showed the Balmer series and very prominent Ca H&K lines, which excluded a white dwarf. To improve the classification and for a subsequent quantitative spectral analysis, we obtained another set of six single spectra ($R = 5000$ –7500, $\lambda = 3000$ –25 000 Å) with XSHOOTER mounted at the ESO Very Large Telescope (VLT) on May 8, 2014. While those spectra have been taken with narrow slits 0.8–0.9 arcsec, we obtained an additional spectrum with

⁴ vizier.u-strasbg.fr/viz-bin/VizieR

⁵ <http://www.aavso.org/download-apass-data>

a wide slit of 5.0 arcsec to minimise slit losses and achieve an absolute flux calibration over the full wavelength range. Since the seeing at that time was ~ 0.9 arcsec, the resolution of this spectrum is similar to the rest of this dataset.

5.1. Spectral classification

The XSHOOTER spectra (see Fig. 6) revealed weak metal lines indicating that WISE J0725–2351 is a metal poor star of spectral type F. For further reference we use the list of Gaia FGK benchmark stars for metallicity (Jofré et al. 2014, their Table 1), which includes only three stars with $[Fe/H] < -2$.

We retrieved XSHOOTER spectra of two of them from the ESO archive. The spectrum of the bluest star, HD 84937 (listed in Jofré et al. 2014 with $[Fe/H] = -2.08$, $T_{\text{eff}} = 6275$ K, $\log g = 4.11$), is very similar to that of WISE J0725–2351. The second best match from their table is HD 140283 ($[Fe/H] = -2.41$, $T_{\text{eff}} = 5720$ K, $\log g = 3.67$). These two comparison stars are also included as the second- and third-brightest objects in the SIMBAD sample of sdF subdwarfs with trigonometric parallaxes shown in Figs. 1 and 2. SIMBAD gives very large numbers of references (>500) for both objects and lists a spectral type of sdF5 for HD 84937, but sdF3 for the cooler HD 140283. Although both objects have been used as well-investigated standards for a long time, the catalogue of Skiff (2014) lists a large variety of spectral types between early- and late-F (or -sdF) types (in the case of HD 140283 even G-types and luminosity class IV) from publications between 1966 and 1999 (in some earlier works they were also classified as A-type (sub)dwarfs). According to its already mentioned relatively small $\log g$ and the recent interferometric radius measurement of 2.21 ± 0.08 solar radii (Creevey et al. 2014), HD 140283 is a metal-poor subgiant rather than a subdwarf. Even HD 84937, for which a spectral type of sdF5 or F5VI is given in all recent catalogues listed in VizieR, is described by VandenBerg et al. (2014) as a metal-poor turnoff star just beginning its subgiant branch evolution. All these discrepancies indicate that there are problems with a spectroscopic classification scheme at the warm end of the cool subdwarf sequence. Therefore, we assign only a preliminary spectral type of sdF5: to WISE J0725–2351.

5.2. Radial velocity curve

To search for radial velocity variations another set of medium-resolution spectra ($R \approx 2200$, $\lambda = 4450\text{--}5110\text{\AA}$) were obtained at 13 epochs with the EFOSC2 spectrograph in February 2014. Radial velocities (v_{rad}) were measured by fitting a set of mathematical functions (polynomial, Lorentzian, and Gaussian) to the Balmer lines of the EFOSC2 and XSHOOTER spectra using the FITSB2 routine (Napiwotzki et al. 2004). No significant variations of v_{rad} were measured within the EFOSC2 dataset. The radial velocity is constant at 230 ± 9 km/s (see Fig. 4), where the average 1σ error of the single measurements is adopted as uncertainty. The XSHOOTER spectra in the UVB arm show no variability in v_{rad} within ~ 45 min. The radial velocity of 238.9 ± 1.8 km/s is perfectly consistent with that derived from the EFOSC2 dataset. Since no variations of v_{rad} have been measured on timescales of hours, days, and months, we can exclude a close stellar companion if its orbit is not aligned in the plane of the sky.

Table 3. Derived parameters of WISE J0725–2351

Parameter	WISE J0725–2351
Spectral type	sdF5.0:
T_{eff} [K]	6250 ± 100
$\log g$	4.0 ± 0.2
$[Fe/H]$	-2.0 ± 0.2
d_{phot} [pc]	430^{+120}_{-90}
v_{tan} [km/s]	544^{+151}_{-114}
v_{rad} [km/s]	$+238.9 \pm 1.8$
v_{grf} [km/s]	460^{+135}_{-102}
u [km/s]	-247^{+95}_{-60}
v [km/s]	-165^{+57}_{-43}
w [km/s]	-351^{+85}_{-63}

6. Quantitative spectral analysis

We carried out a quantitative spectral analysis of the XSHOOTER spectra using grids of Kurucz LTE model atmospheres (Castelli & Kurucz 2004, Munari et al. 2005).

In the first step we compared the flux-calibrated XSHOOTER spectrum to synthetic spectra for an adopted metallicity of $[Fe/H] = -2.0$, an alpha enrichment of $[\alpha/Fe] = +0.4$ with a mixing-length parameter of 1.25, and different effective temperatures and gravities (see Fig. 5). The best match is found for $T_{\text{eff}} = 6250$ K and a surface gravity of $\log g = 4.0$. As can be seen, the Paschen continuum is a good temperature indicator, whereas the gravity can be derived from the Balmer jump. We adopted uncertainties of $\delta T_{\text{eff}} = 100$ K and $\delta \log g = 0.2$ dex. Thereafter, we kept the gravity fixed and proceeded to the analysis of the high resolution XSHOOTER spectrum. We used the program FITSB2 (Napiwotzki et al. 2004) to fit the Balmer lines H_{β} , H_{γ} , and H_{δ} as well as several wavelength ranges covering important spectral lines (see VandenBerg et al. 2014). Effective temperature and metallicity (with given $[\alpha/Fe] = +0.4$) were derived to $T_{\text{eff}} = 6250 \pm 100$ K and $[Fe/H] = -2.0 \pm 0.2$. A comparison of the best-match model spectrum to the XSHOOTER observation is shown in Fig. 6. The effective temperature derived is consistent with that derived from the flux-calibrated spectrum. The errors of our final physical parameters (Table 3, top rows) were estimated by visual inspection of all fits of different model spectra to the observed XSHOOTER spectrum.

To verify our procedure, we also studied the halo star HD 84937 in the same way. We obtained XSHOOTER spectra from the ESO archive. A detailed quantitative spectral analysis has recently been carried out by VandenBerg et al. (2014), which resulted in $T_{\text{eff}} = 6408$ K, $\log g = 4.05$, $[Fe/H] = -2.08$ and $[\alpha/Fe] = +0.38$ (in good agreement with the parameters in Jofré et al. 2014.) Applying the same procedure as for WISE J0725–2351 to the XSHOOTER spectra of HD 84937, we confirm the results of VandenBerg et al. (2014) to within error limits. In particular, the surface gravity derived here from the Balmer jump is consistent with that determined by VandenBerg et al. (2014) from mass, T_{eff} and bolometric corrections. In conclusion, WISE J0725–2351 is probably a halo turnoff star similar in composition, mass, and age to HD 84937.

7. Photometric distance and space velocity

Finally, we inspected the spectral energy distribution (SED) by making use of the photometric measurements summarised in Table 2 thereby covering the SED from the near-ultraviolet (NUV) (GALEX) to the far-infrared (FIR) (WISE). We used the cali-

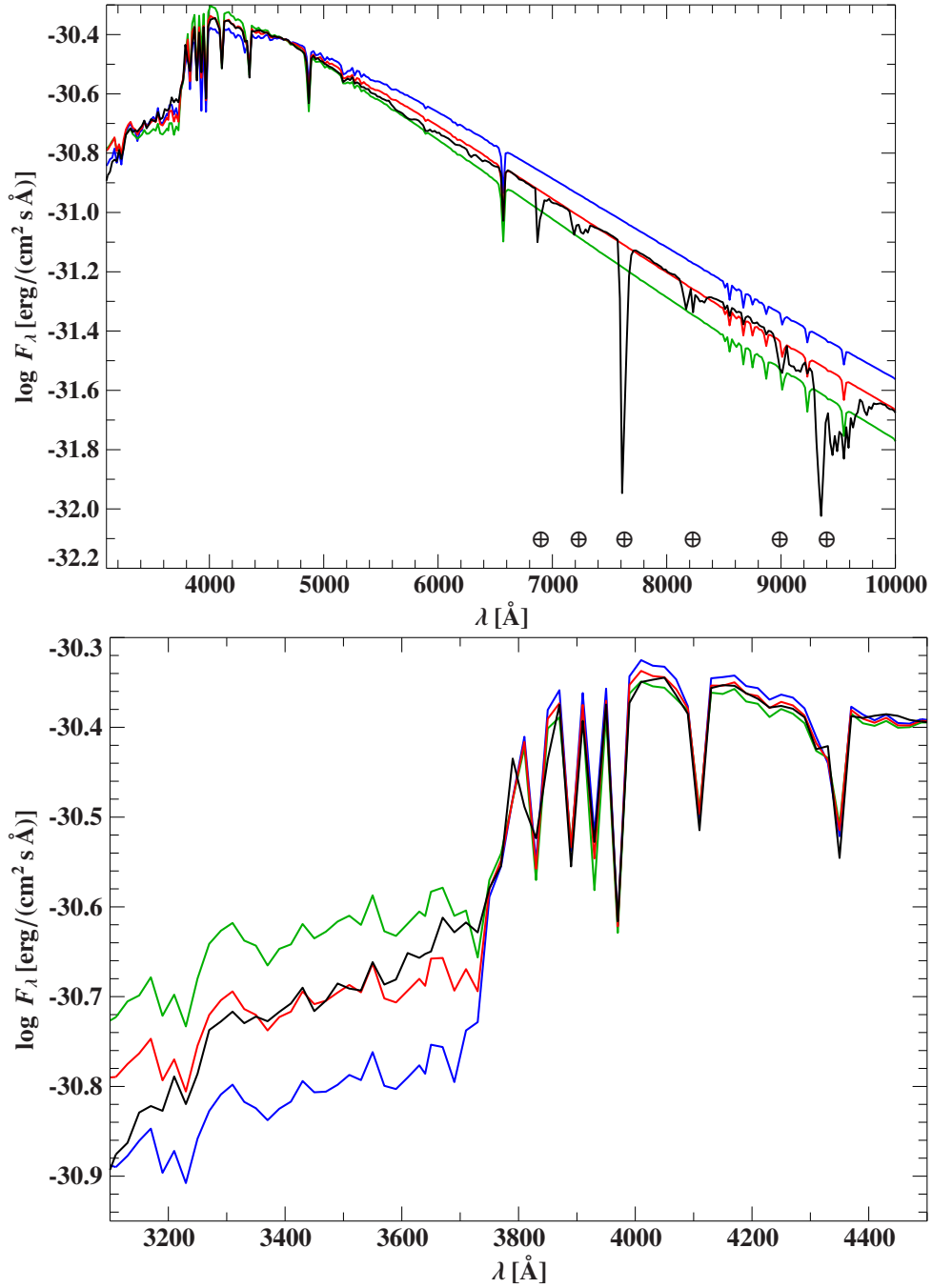


Fig. 5. XSHOOTER spectrum of WISE J0725–2351 (black; telluric absorption bands are marked by \oplus) compared to a synthetic spectrum with $[\text{Fe}/\text{H}]=-2.0$, $T_{\text{eff}}=6250$ K and $\log g=4.0$ (red). **Top:** for the full wavelength interval additional synthetic spectra with changed temperature $T_{\text{eff}}=6500$ K (green) and 6000 K (blue) are shown. **Bottom:** for the region of the Balmer jump, the additional synthetic spectra show the effect of changing gravity to $\log g=4.5$ (green) and $\log g=3.5$ (blue).

brations of Morrissey et al. (2007), Pickles & Depagne (2010), Cohen et al. (2003), and Jarrett et al. (2011) to convert magnitudes to fluxes. We adopted the atmospheric parameters derived above and included interstellar absorption. The magnitudes were dereddened using the extinction coefficients of Yuan et al. (2013). The synthetic spectra were scaled to match the K_s -band flux. The best match is derived for a colour excess of $E(B-V)=0.03$ mag, indicating very little extinction to WISE J0725–2351. As can be seen from Fig. 7, the synthetic spectrum matches the observed SED perfectly. The fit also allowed us to determine the distance because the angular diameter was derived from the scaling factor. In addition, the stellar radius can be derived from the gravity

and the stellar mass. We adopted $0.8 M_{\odot}$. Accordingly, the distance was determined as 430^{+120}_{-90} pc, where the uncertainties stem from the uncertainty of the gravity.

Because of very good agreement in the physical parameters of our target with those of HD 84937, we also used the relatively well-known *Hipparcos* distance (72.8 ± 4.1 pc according to van Leeuwen 2007) of HD 84937 for an additional photometric distance estimate of WISE J0725–2351. Using the $BVJHK_s w2w3$ photometry, and conservatively assuming the absolute magnitude uncertainties of about ± 0.2 mag, we estimated a mean photometric distance of 391 ± 39 pc. If we prefer the smaller and more accurate parallax of HD 84937 recently measured by Van-

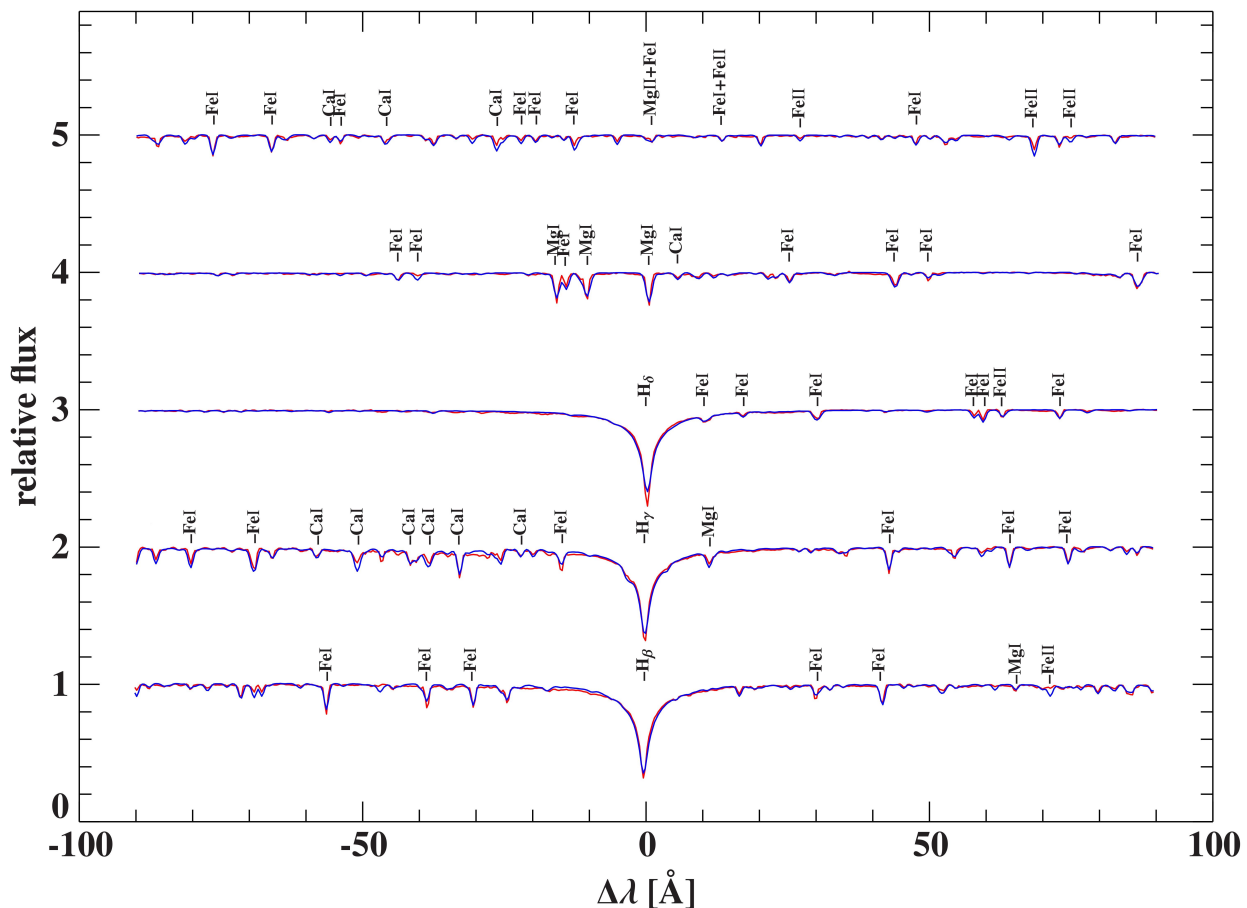


Fig. 6. XSHOOTER spectrum of WISE J0725–2351 (red) at higher resolution for the regions of the Balmer lines H_β , H_γ , and H_δ and other important spectral lines. The best-fit model spectrum with $T_{\text{eff}}=6250$ K, $\log g=4.0$, $[\text{Fe}/\text{H}]=-2.0$, and $[\alpha/\text{Fe}]=+0.4$ is shown in blue.

denBerg et al. (2014) using the *Hubble Space Telescope*, the distance of WISE J0725–2351 increases to 439 ± 44 pc. These distance estimates based on the assumption that WISE J0725–2351 is just a more distant copy of HD 84937 and neglecting possible differences in the reddening of the two objects are in very good agreement with the distance derived from the SED. We adopt the distance derived from the SED with its larger errors until the gravity of WISE J0725–2351 will be determined with higher accuracy.

With this distance, the proper motion of WISE J0725–2351 results in an extremely large tangential velocity (Table. 3). This is however still consistent with the majority of the known sdF/sdG subdwarfs having tangential velocities between 100 and up to about 500 km/s (Fig. 2, bottom). Despite its larger uncertainty, the tangential velocity is clearly larger than the radial velocity. The object is located at $l \sim 238.0^\circ$, $b \sim -3.6^\circ$, right in the Galactic plane.

We calculated the Galactocentric kinematic properties of WISE J0725–2351 (bottom rows in Table 3) based on the input parameters given in Tables 1 and 3 (middle part) following the equations of Randall et al. (2014) by varying the position and velocity components within their respective errors by applying a Monte Carlo procedure with a depth of 100000. The distance of the sun from the Galactic center was assumed to be 8.4 kpc. According to Schönrich et al. (2010) its motion relative to the local standard of rest (LSR) is $v_{x\odot}=11.1$ km/s, $v_{y\odot}=12.24$ km/s, $v_{z\odot}=7.25$ km/s, and the velocity of the LSR is $v_{\text{LSR}}=242$ km/s, as predicted by Model I of Irigang et al. (2013). We derived a Galactic restframe velocity of WISE J0725–

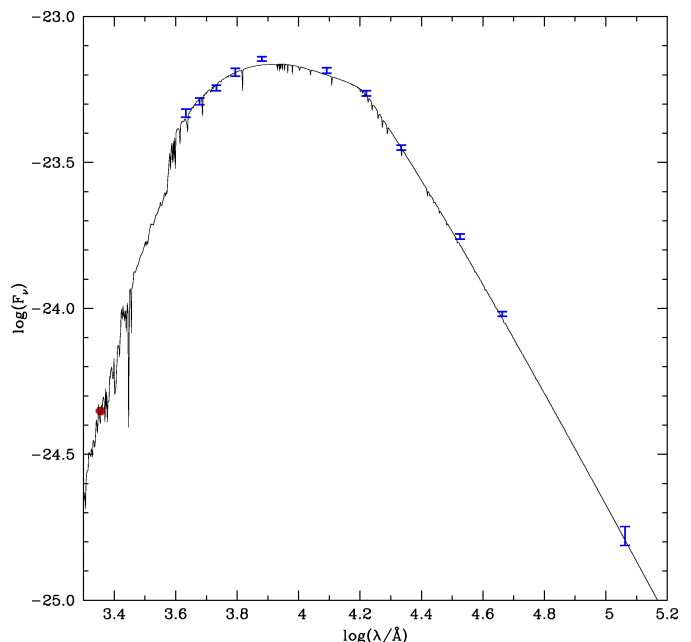


Fig. 7. Comparison of the observed flux distribution of WISE J0725–2351 derived from the photometry listed in Table 2 and dereddened for $E(B - V)=0.03$ mag to a synthetic spectrum with $T_{\text{eff}}=6250$ K, $\log g=4.0$ and $[\text{Fe}/\text{H}]=-2.0$. The GALEX NUV flux is displayed as a red hexagon for clarity. Its uncertainty is much lower than the symbol size.

2351 $v_{grf}=460^{+135}_{-102}$ km/s, a Galactic radial velocity component $u=-247^{+95}_{-60}$ km/s, a rotational component $v=-165^{+57}_{-43}$ km/s, and a component $w=-351^{+85}_{-63}$ km/s perpendicular to the Galactic plane. These values imply that the star is a halo star on a retrograde bound orbit (about 9% of the simulations led to unbound orbits) that is passing close by the Galactic disc. Its location in a u - v diagram (see e.g. Fig. 2 in Pauli et al. 2006 for WDs, or Fig. 10 in Tillich et al. 2011 for sdB stars) is clearly outside the limits of the thin and thick disc populations. The w component is very large compared to those of M-type halo subdwarfs in Lépine et al. (2003).

8. Discussion and conclusions

We have discovered a new F-type subdwarf (sdF5:) or metal-poor turnoff star, which is very similar to the case of HD 84937, one of the best-known representatives of this elusive class of objects. The new object, WISE J0725–2351, is currently located at about 400 pc from the sun in the Galactic plane, but crosses it at a high speed typical of an extreme Galactic halo object. The velocity component perpendicular to the plane is very large, and the negative Galactic rotational velocity component indicates a retrograde orbit. We expect WISE J0725–2351 to be roughly the same age as HD 84937, for which Vandenberg et al. (2014) determined an age of about 12 Gyr. With its $\log T_{\text{eff}}=3.796$ and the (uncertain) absolute magnitude of $M_V=3.89$, WISE J0725–2351 would be placed in between HD 84937 and HD 19445, but closer in absolute magnitude to HD 84937, as shown in Fig. 1 of Vandenberg et al. (2014). These authors measured $[Fe/H]=-2.03$, $T_{\text{eff}}=6136$ K, and $\log g=4.43$ for HD 19445, a well-measured subdwarf about ~ 1 mag below the turnoff at the metallicity of $[Fe/H]\sim -2$, which they included in their analysis to check the isochrones. According to our gravity measurement for WISE J0725–2351, it seems more likely to be a metal-poor turnoff star than a normal F-type subdwarf.

We classify WISE J0725–2351 as a relatively metal-poor star at the boundary to the class of extremely metal-poor stars. Its colours meet only three out of seven selection criteria for the best and brightest metal-poor stars as suggested by Schlafman & Casey (2014). In particular, its $J-H=0.27$ and $J-w2=0.35$ are not as red as the required limits (0.45 and 0.5, respectively), whereas its $w1-w2=-0.03$ and $B-V=0.43$ are in the right ranges. In that respect, WISE J0725–2351 is again similar to the benchmark metal-poor subdwarf or turnoff star HD 84937. The other two metal-poor Gaia benchmark stars from Jofré et al. (2014), the already mentioned slightly cooler subgiant HD 140283 and especially the much cooler giant HD 122563 ($[Fe/H]=-2.59$, $T_{\text{eff}}=4608$ K, $\log g=1.61$), show larger $J-H$ and $J-w2$ colour indices so that the latter fulfils most of the Schlafman & Casey (2014) preconditions. Nevertheless, we think that WISE J0725–2351 is a good target for higher resolution spectroscopy and the analysis of elemental abundances.

Acknowledgements. E.Z. and C.H. acknowledge support by the Deutsche Forschungsgemeinschaft (DFG) through grants HE 1356/45-2 and HE 1356/62-1, respectively. We thank U. Munari for providing us with his synthetic spectra of high spectral resolution. This research has made use of the National Aeronautics and Space Administration (NASA)/Infrared Processing and Analysis Center (IPAC) Infrared Science Archive, which is operated by the Jet Propulsion Laboratory (JPL), California Institute of Technology (Caltech), under contract with the NASA, of data products from WISE, which is a joint project of the University of California, Los Angeles, and the JPL/Caltech, funded by the NASA, and from 2MASS. We have extensively used SIMBAD and VizieR at the CDS/Strasbourg. We thank the anonymous referee for a prompt report.

References

- Allende Prieto, C., Fernández-Alvar, E., Schlesinger, K. J., et al. 2014, A&A, 568, A7
- Burgasser, A. J., Lépine, S., Lodieu, N., et al. 2009, 15th Cambridge Workshop on Cool Stars, Stellar Systems, and the Sun, 1094, 242
- Castelli, F., & Kurucz, R. L. 2004, arXiv:astro-ph/0405087
- Chamblérain, J. W., & Aller, L. H. 1951, ApJ, 114, 52
- Cohen, M., Wheaton, W. A., Megeath, S. T. 2003, AJ, 126, 1090
- Creevey, O., Thévenin, F., Berio, P., et al. 2014, arXiv:1410.4780
- Cushing, M. C., Looper, D., Burgasser, A. J., et al. 2009, ApJ, 696, 986
- Drilling, J. S., Jeffery, C. S., Heber, U., Moehler, S., & Napiwotzki, R. 2013, A&A, 551, A31
- Egret, D., Didelon, P., McLean, B. J., Russell, J. L., & Turon, C. 1992, A&A, 258, 217
- ESA 1997, HIPPARCOS and Tycho catalogues, ESA-SP 1200
- Girard, T. M., van Altena, W. F., Zacharias, N., et al. 2011, AJ, 142, 15
- Gizis, J. E. 1997, AJ, 113, 806
- Gontcharov, G. A., Bajkova, A. T., Fedorov, P. N., & Akhmetov, V. S. 2011, MNRAS, 413, 1581
- Greenstein, J. L. 1954, PASP, 66, 126
- Hambly, N. C., MacGillivray, H. T., Read M. A., et al. 2001a, MNRAS, 326, 1279
- Hambly, N. C., Irwin, M. J., & MacGillivray, H. T. 2001b, MNRAS, 326, 1295
- Hambly, N. C., Davenhall, A. C., Irwin, M. J., & MacGillivray, H. T. 2001c, MNRAS, 326, 1315
- Hambly, N. C., Henry, T. J., Subasavage, J. P., Brown, M. A., & Jao, W.-C. 2004, AJ, 128, 437
- Høg, E., Fabricius, C., Makarov, V. V., et al. 2000, A&A, 355, L27
- Irrgang, A., Wilcox, B., Tucker, E., & Schiefelbein, L. 2013, A&A, 549, AA137
- Jao, W.-C., Henry, T. J., Beaulieu, T. D., & Subasavage, J. P. 2008, AJ, 136, 840
- Jarrett, T. H., Cohen, M., Masci, F., et al. 2011, ApJ, 735, 112
- Jofré, P., Heiter, U., Soubiran, C., et al. 2014, A&A, 564, A133
- Kirkpatrick, J. D., Schneider, A., Fajardo-Acosta, S., et al. 2014, ApJ, 783, 122
- Lépine, S., Rich, R. M., & Shara, M. M. 2003, AJ, 125, 1598
- Lépine, S. 2005, AJ, 130, 1247
- Lépine, S., & Shara, M. M. 2005, AJ, 129, 1483
- Lépine, S., Rich, R. M., & Shara, M. M. 2007, ApJ, 669, 1235
- Lépine, S. 2008, AJ, 135, 2177
- Lépine, S., & Gaidos, E. 2013, Astronomische Nachrichten, 334, 176
- Lodieu, N., Espinoza Contreras, M., Zapatero Osorio, M. R., et al. 2012, A&A, 542, A105
- Luhman, K. L. 2013, ApJ, 767, L1
- Luhman, K. L. 2014a, ApJ, 781, 4
- Luhman, K. L. 2014b, ApJ, 786, L18
- Luhman, K. L., & Sheppard, S. 2014, ApJ, 787, 126
- Luyten, W. J. 1979a, LHS Catalogue: a catalogue of stars with proper motions exceeding 0.5" annually, University of Minnesota, Minneapolis
- Luyten W. J. 1979b, New Luyten Catalogue of Stars with Proper Motions Larger than Two Tenths of an Arcsecond, Univ. Minnesota, Minneapolis
- Mason, B. D., Wycoff, G. L., Hartkopf, W. I., Douglass, G. G., & Worley, C. E. 2001, AJ, 122, 3466
- Monet, D. G., Levine, S. E., Canzian, B., et al. 2003, AJ, 125, 984
- Morrissey, P., Conrow, T., Barlow, T. A., et al. 2007, ApJ Suppl. Ser., 173, 682
- Muñoz, J. L., & Evans, D. W. 2014, Astronomische Nachrichten, 335, 367
- Munari, U., Sordo, R., Castelli, F., & Zwitter, T. 2005, A&A, 442, 1127
- Napiwotzki, R., Yungelson, L., Nelemans, G. et al. 2004, ASP Conf. Ser., 318, 402
- Parker, Q. A., Philipps, S., Pierce, M. J., et al. 2005, MNRAS, 362, 689
- Pauli, E.-M., Napiwotzki, R., Heber, U., Altmann, M., & Odenkirchen, M. 2006, A&A, 447, 173
- Pickles, A., & Depagne, É. 2010, PASP, 122, 1437
- Pokorny, R. S., Jones, H. R. A., Hambly, N. C., & Pinfield, D. J. 2004, A&A, 421, 763
- Rajpurohit, A. S., Reylé, C., Allard, F., et al. 2014, A&A, 564, A90
- Randall, S., Bagnulo, S., Ziegerer, E., Geier, S., Fontaine, G. 2014, A&A, submitted
- Reylé, C., Scholz, R.-D., Schultheis, M., Robin, A. C., & Irwin, M. 2006, MNRAS, 373, 705
- Röser, S., Schilbach, E., Schwan, H., et al. 2008, A&A, 488, 401
- Schilbach, E., Röser, S., & Scholz, R.-D. 2009, A&A, 493, L27
- Schlaufman, K. C., & Casey, A. R. 2014, ApJ, 797, 13
- Schönrich, R., Binney, J., & Dehnen, W. 2010, MNRAS, 403, 1829
- Scholz, R.-D., Irwin, M., Ibata, R., et al. 2000, A&A, 353, 958
- Scholz, R.-D., Lodieu, N., & McCaughrean, M. J. 2004, A&A, 428, L25
- Skiff, B. A. 2014, CDS/ADC Collection of Electronic Catalogues, 1, 2023, <http://cdsbib.u-strasbg.fr/cgi-bin/cdsbib?2014yCat....1.2023S>
- Skrutskie, M. F., Cutri, R. M., Stiening, R., et al. 2006, AJ, 131, 1163
- Thome J. M. 1892, Resultados del Observatorio Nacional Argentino, part I: -22deg to -32deg
- Tillich, A., Heber, U., Geier, S., et al. 2011, A&A, 527, AA137
- Urban, S. E., Corbin, T. E., Wycoff, G. L., et al. 1998, AJ, 115, 1212
- Vandenberg, D. A., Bond, H. E., Nelan, E. P., et al. 2014, ApJ, 792, 110
- van Leeuwen, F. 2007, A&A, 474, 653
- Winters, J. G., Henry, T. J., Lurie, J. C., et al. 2014, AJ, 149, 5
- Wright, E. L., Eisenhardt, P. R. M., Mainzer, A. K., et al. 2010, AJ, 140, 1868
- Wright, E. L., Kirkpatrick, J. D., Gelino, C. R., et al. 2014, AJ, 147, 61
- Yuan, H. B., Liu, X. W., & Xiang, M. S. 2013, MNRAS, 430, 2188
- Zacharias, N., Finch, C. T., Girard, T. M., et al. 2013, AJ, 145, 44
- Zhang, Z. H., Pinfield, D. J., Burningham, B., et al. 2013, European Physical Journal Web of Conferences, 47, 6007